Groundwater flow due to a nonlinear wave set-up on a permeable beach

Anna Przyborska

Institute of Oceanology,
Polish Academy of Sciences,
Powstańców Warszawy 55, 81–712 Sopot, Poland;

e-mail: aniast@poczta.onet.pl

Abstract

Water flow through the beach body plays an important role in the biological status of the organisms inhabiting the beach sand. For tideless seas, the groundwater flow in shallow water is governed entirely by the surface wave dynamics on the beach. As waves propagate towards the shore, they become steeper owing to the decreasing water depth and at some depth, the waves lose their stability and start to break. When waves break, their energy is dissipated and the spatial changes of the radiation stress give rise to changes in the mean sea level, known as the set-up. The mean shore pressure gradient due to the wave set-up drives the groundwater circulation within the beach zone. This paper discusses the circulation of groundwater resulting from a nonlinear set-up. The circulation of flow is compared with the classic Longuet-Higgins (1983) solution and the time series of the set-up is considered for a 24 h storm. Water infiltrates into the coastal aquifer on the upper part of the beach near the maximum run-up and exfiltration occurs on the lower part of the beach face near the breaking point.

1. Introduction

Water dynamics in the coastal zone of tideless seas is determined by the energy transmitted in waves and currents, the decisive part being

by surface waves impacting on the beach. Waves from the deep sea change their shape and become steeper owing to the decreasing water depth. At some depth, the waves lose their stability and start to break, running up and down on the beach surface, whereby a certain amount of water seeps into the permeable beach, generating a complex circulation in the porous medium. When waves break, their energy is dissipated and the spatial changes of the radiation stress give rise to changes in the mean sea level, known as the set-up.

In the classic paper by Longuet-Higgins & Stewart (1964) the set-up was calculated using the linear model based on the shallow-water equation. Longuet-Higgins (1983) demonstrated that the mean onshore pressure gradient due to wave set-up drives a groundwater circulation within the beach zone. Water infiltrates into the coastal aquifer on the upper part of the beach near the maximum run-up, and exfiltration occurs on the lower part of the beach face near the breaking point. This paper presents a theoretical attempt to predict the groundwater circulation induced by the nonlinear wave set-up.

2. Material and methods

2.1. Theory

The proposed solution is based on the theoretical concept of multiphase flows in the porous media of a beach. The basic value determined experimentally or calculated in the model is pore pressure in the beach sand. The theoretical model is based on the Biot's theory, which takes into account the deformation of the soil skeleton, the content of the air/gas dissolved in pore water, and the change in volume and direction of the pore water flow (Biot 1956), resulting from changes in vertical gradients and vertical pore pressure. It is assumed that the deformations of the soil skeleton conform to the law of linear elasticity. The major issue being examined is the fact that when waves break, they inject air and gases into the porous medium. In addition, gases are produced by organisms living in the sand. Hence, we are dealing with a three-phase medium consisting of a soil skeleton, pore water and gas/air. As a result, the elastic modulus of pore water E'_w depends on the degree of water saturation with air (Verruijt 1969).

Analysis of the results of a laboratory experiment showed that in the case where fine sand is saturated with air or gas, the rigidity of the soil is much greater than that of the pore water. The equation for the water pressure in the soil pores can be written in the form (Massel et al. 2005):

$$\bigtriangledown^2 p - \frac{\gamma n}{K_f E'_w} \frac{\partial p}{\partial t} = 0, \tag{1}$$

where

K_f	–	coefficient of permeability,
$\gamma = \rho g$	–	specific gravity of water,
n	–	porosity of the porous medium,
E'_w	–	bulk modulus of pore water,
p	–	pore pressure.

The solution of equation (1) is the following function:

$$p(x, z, t) = \Re \left\{ \frac{\rho_w g}{\cosh(kh)} \left| \frac{\cosh[\psi(z + h_n)]}{\cosh[\psi(h_n - h)]} \right| \exp[i\varphi] \right\} \zeta(x, t), \qquad (2)$$

where

$$\psi^2 = k^2 \left(1 - i \frac{n\gamma\omega}{k^2 K_f E'_w} \right), \qquad (3)$$

where n is a measure of the porosity (the ratio of free pore volume to total volume), $\Re$ is the real part of a complex number. According to the solution, the presence of air in the porous medium causes a phase delay φ between the deflection of the free surface and the pore pressure.

Massel et al. (2004) showed that the solutions of equations (1) coincide well with the experimental data, and they will be used in the further analysis of the determination of pore pressure. In addition to the pore pressure, the filtration rates in soil pores are also interesting. The components of the groundwater flow velocity vector (u, v) satisfy the following system of equations (Moshagen & Torum 1975):

$$\begin{cases} \frac{\partial u}{\partial t} + u\frac{\partial u}{\partial x} + v\frac{\partial u}{\partial z} = -\frac{1}{n\rho}\frac{\partial p}{\partial x} - \frac{g}{nK_f}u, \\[2mm] \frac{\partial v}{\partial t} + u\frac{\partial v}{\partial x} + v\frac{\partial v}{\partial z} = -\frac{1}{n\rho}\frac{\partial p}{\partial z} - \frac{g}{nK_f}v, \\[2mm] \frac{u}{\rho_w}\frac{\partial \rho}{\partial x} + \frac{v}{\rho_w}\frac{\partial \rho}{\partial z} + \frac{\partial u}{\partial x} + \frac{\partial v}{\partial z} = -\frac{n}{nK_f}\frac{\partial p}{\partial t}. \end{cases} \qquad (4)$$

In the stationary case and after ignoring the non-linear members, components of the velocity vector may be determined from the measurements of pressure with formulas resulting from Darcy's law:

$$\begin{cases} u(x, z, t) = -\frac{K_f}{\rho_w g}\frac{\partial p}{\partial x}, \\[2mm] v(x, z, t) = -\frac{K_f}{\rho_w g}\frac{\partial p}{\partial z}. \end{cases} \qquad (5)$$

From relations (2) and (5), we obtain the following components of the velocity of circulation of ground water caused by a surface wave of height H and frequency ω:

$$u(x, z, t) = \Re \left\{ i\frac{K_f}{n}\frac{kH}{2}\frac{\cosh[\psi(z + h_n)]}{\cosh(kh)\cosh[\psi(h_n - h)]} \exp[i(kx - \omega t)] \right\} \qquad (6)$$

and

$$v(x,z,t) = \Re\left\{\frac{K_f}{n}\frac{\psi H}{2}\frac{\sinh\left[\psi(z+h_n)\right]}{\cosh(kh)\cosh\left[\psi(h_n-h)\right]}\exp\left[i(kx-\omega t)\right]\right\}. \quad (7)$$

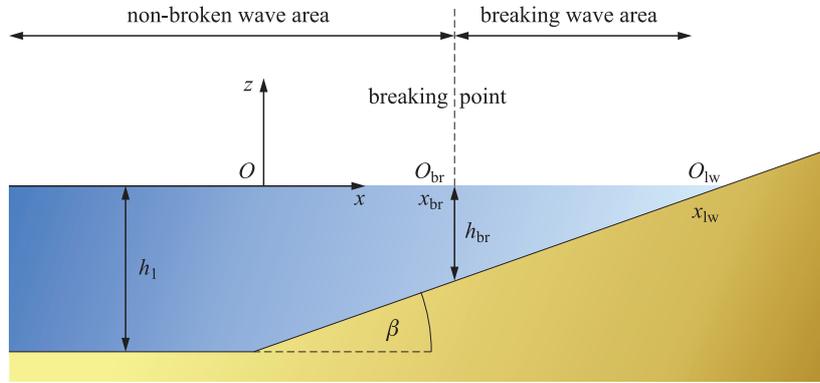The wave number k satisfies the classical dispersion relation:

$$\omega^2 = gh\tanh(kh). \quad (8)$$

2.2. Set-up influences on the groundwater circulation

Let us assume that waves move towards the shore above the bottom of a slope β. The water depth thus satisfies the following relationship:

$$h(x) = h_1 - \beta x, \quad (9)$$

where h_1 is the initial water depth (Figure 1).

Figure 1. Reference scheme

During its transformation on a sloping bottom, a wave changes its parameters: it becomes steeper and at some point in the coastal zone (point O_{br}) the wave breaks. The dynamics before and after the breaking point is different. Therefore, the pressure at the bottom and also the pore water pressure and pore water velocity will depend on the location in relation to the breaking point.

In particular, we should distinguish two zones: the pore pressure in front of the breaking zone and behind the breaking zone (Massel et al. 2004). Experiments on the wave channel in Hannover showed that the pore pressure in front of the breaking zone corresponds directly to the oscillation of the sea surface $\zeta(x,t)$. Behind the breaking zone the pore pressure changes in a different way. In addition to oscillations similar to those of the free sea surface, there is a fixed component of the hydrostatic pressure associated with the elevation of mean sea level $\bar{\zeta}$.

Let us consider separately the two types of pore pressure and the circulation related to them. If we assume that the slope of the bottom in front of the breaking zone is very smooth, which is usually the case on sandy shores, then we can use the solution from equation (1) to determine pore pressure and circulation. The sea depth at the point where the pore pressure is aanalysed is assumed to be locally constant. The wave height at this point is calculated on the basis of H_1 at the initial depth h_1, or the data from observations are used. The following results from the energy conservation flux laws (after ignoring losses caused by bottom friction):

$$\frac{1}{8}\rho g H_1^2 C_g(h_1) = \frac{1}{8}\rho g H^2 C_g(h) \tag{10}$$

and where

$$H(h) = \sqrt{\frac{C_g(h_1)}{C_g(h)}} H_1 \tag{11}$$

and $C_g(h_1)$ and $C_g(h)$ are the group velocities at the points of depths h_1 and h respectively, i.e.

$$C_g(h) = \frac{C}{2}\left[1 + \frac{2kh}{\sinh 2kh}\right], \tag{12}$$

where $C = \frac{L}{T} = \frac{\omega}{k}$ is the phase velocity of the wave. The resulting pressure p and the velocity u and v at the point of depth h are given by formulas (2), (6), (7).

Under such assumed conditions of changing depth, the speed of propagation C, the group velocity C_g and the length L of the waves are decreasing. According to the principle of conservation of energy the wave height H is increasing. However, the spreading waves, sooner or later, dissipate as a result of their breaking. The factor controlling wave breaking is the steepness s, defined as the ratio of wave height H to wave length L, $s = \frac{H}{L}$ (Holthuijsen 2007). This process occurs in different ways, depending on the wave parameters and the slope of the bottom.
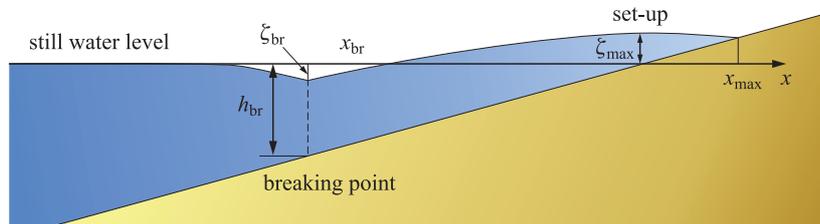
Figure 2. The mean sea level elevation (set-up) in a shoreline area

Let us demonstrate briefly the mechanism by which the mean sea level elevation $\bar{\zeta}$ changes.

Immediately before the wave breaking point (Figure 2), the average water level changes slightly (a very small set-down). As a result of the wave breaking, the wave height decreases and a negative wave energy gradient $\sim \frac{dH^2}{dx} < 0$ is created. This gradient is compensated by the rising mean sea level $\bar{\zeta}$.

2.2.1. Linear set-up mechanism

Longuet-Higgins & Stewart (1962, 1964) showed that when the wave-motion lasts long enough, the ordinate $\bar{\zeta}$ of the mean sea level elevation set-up(x) satisfies the following equation:

$$\frac{dS_{xx}(x)}{dx} + \rho g \left(h + \bar{\zeta}(x) \right) \frac{d\bar{\zeta}(x)}{dx} = 0, \tag{13}$$

where S_{xx} is a component of the radiation stress tensor in the direction perpendicular to the shore, associated with wave energy:

$$S_{xx} = \frac{3}{2} E, \tag{14}$$

where $E = \frac{1}{8} \rho g H^2$.

Before the breaking zone, where waves do not break and we have no energy loss, changes in the mean sea level are due only to the changing depth. In this case we have:

$$\bar{\zeta} = -\frac{1}{8} \frac{kH^2}{\sinh(2kh)}. \tag{15}$$

Particularly in the immediate vicinity of the breaking zone, for a very small depth, when $\sinh(2kh) \approx 2kh$, from (15) we obtain:

$$\zeta_{br} = -\frac{1}{16} \gamma_{br} H_{br}, \tag{16}$$

where H_{br} is the height of the wave at the breaking point.

Since we know where a wave begins to break down, the coefficient $\gamma \approx 0.8$ which gives a mean decrease of water level $\bar{\zeta}_{br}$ of $4-5\%$ of local depth. When the water depth $h(x) = h_1 - \beta x$, the height of the mean sea level elevation is also a linear function of distance.
In the light of this, we thus have:

$$\bar{\zeta}(x) = \bar{\zeta}_{br} + \frac{3}{8} \gamma_{br}^2 \left(1 + \frac{3}{8} \gamma_{br}^2 \right)^{-1} [h_{br} - h(x)]. \tag{17}$$

The maximum elevation of the mean water level set-up to the coastline, where $h(x) = 0$, takes the following form:

$$\bar{\zeta}_{\max} = \bar{\zeta}_{br} + \frac{3}{8} \gamma_{br}^2 \frac{1}{1 + \frac{3}{8} \gamma_{br}^2} h_{br}, \tag{18}$$

which for very small depths, after taking (16) into account, gives:

$$\bar{\zeta}_{\max} \approx \frac{5}{16}\gamma_{br}. \tag{19}$$

2.2.2. Nonlinear set-up mechanism

Dally et al. (1985) showed that after a wave has broken, its height $H(x)$ over a sloping bottom changes as follows:

$$\frac{H(x)}{H_{br}} = \left(\left(\frac{h(x)}{h_{br}} \right)^{\frac{K}{\beta}-\frac{1}{2}} (1+\alpha) - \alpha \left(\frac{h(x)}{h_{br}} \right)^2 \right)^{\frac{1}{2}}, \tag{20}$$

where

$$\alpha = \frac{K\Gamma^2}{\beta \left(\frac{5}{2} - \frac{K}{\beta} \right) \left(\frac{H}{h} \right)_{br}^2}, h(x) = h_{br} - \beta x. \tag{21}$$

K and Γ are empirical coefficients.

This model is not valid in the immediate vicinity of a coastline, where the depth tends to zero, as at a depth of $h = 0$, the wave height is zero. Under real conditions in the immediate vicinity of a coastline, waves run up and down the beach surface. Let us consider first the function of mean sea level elevation when the only parameter dependent on the external factors is the parameter $\gamma = \left(\frac{H}{h} \right)_{br}$.

When $\alpha = -1$, from (20), we obtain the following approximate relationship:

$$H(x) = \left(\frac{H}{h} \right)_{br} h(x) = \gamma_{br} h(x). \tag{22}$$

In practice, the value of parameter $\gamma_{br} \approx 0.7 - 0.8$.

By substituting (22) in formula (14) we obtain:

$$S_{xx} \approx \frac{3}{16}\rho g \gamma_{br}^2 \left(h + \bar{\zeta} \right)^2. \tag{23}$$

In the general case, the elevation of the mean sea level set-up $\bar{\zeta}(x)$ is not a linear function of x. Note that if instead of equation (22) we assume relation (20), the solution of equation (13) results in a nonlinear (as a function of distance) variability of the mean sea level elevation (Dally et al. 1985):

$$\frac{d\bar{\zeta}(x)}{dx} = -\frac{3}{16} \frac{1}{h(x) + \bar{\zeta}(x)} \frac{dH^2(x)}{dx^2}. \tag{24}$$

Figure 3 compares the mean sea level elevation set-up using the linear approximation (relation 17) and the nonlinear approximation (24). During a controlled large-scale laboratory experiment carried out in the Large Wave
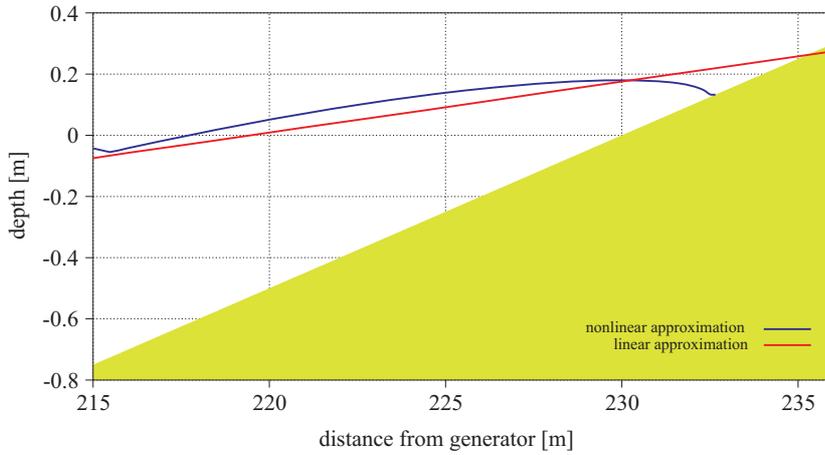
Figure 3. Mean sea level elevation – comparison of the linear and nonlinear approximation

Channel in Hannover, a data set was gathered which compares better with the nonlinear set-up (Massel et al. 2005).

3. Results and discussion

The distance shown on the horizontal axis is the distance in metres for coastal areas, reflected by the beach heaped up in the GWK laboratory in Hannover (Figure 4), where initially, the bottom was flat. Re-profiling into the bottom at an angle $\beta = 1/20$ starts at the point of 150 [m] from the beginning of the channel laboratory, and 230 [m] is the point of intersection of the sea water level with the seabed. '0' is beginning of the
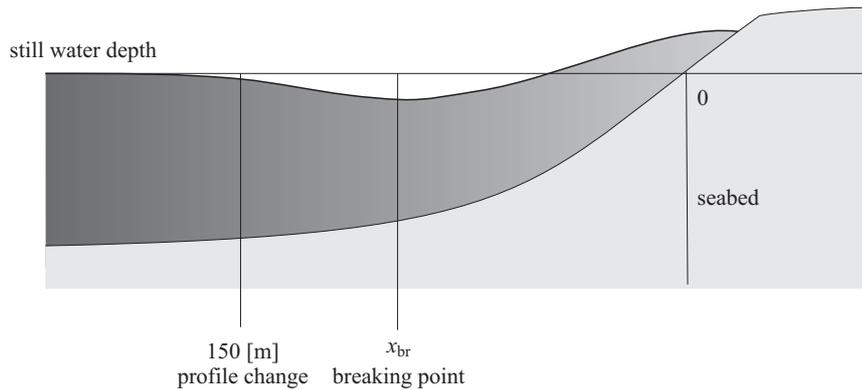
Figure 4. Seabed used for the calculation of examples

wave channel, the point where waves are generated. This notation has been retained to maintain consistency with the work by Massel et al. (2004).

Elevation of the mean sea level is dependent on the characteristics of the wave arriving from the open sea.

3.1. Temporal change in nonlinear set-up

Let us consider, therefore, changes in the mean sea level elevation during during several hours of a storm. Let us assume that as storm waves approach the costal zone, their height $H_0(t)$ changes over deep water according to the following formula:

$$H_0(t) = \left\{ 1 + \cos\left[2\pi\left(\frac{t}{24} - \frac{1}{2}\right)\right] + H_0(t_0) \right\}, \tag{25}$$

where the height $H_0(t_0) = 0.3$ [m]. Let the wave period $T = 6$ [s] and the bottom slope $\beta = 1/20$ the duration of the storm is 24 hours.

Depending on the height of the wave approaching the shore, the width of the surf zone changes. Figure 5 shows the changes of $H_0(t)$ in time during a 24-hour storm.
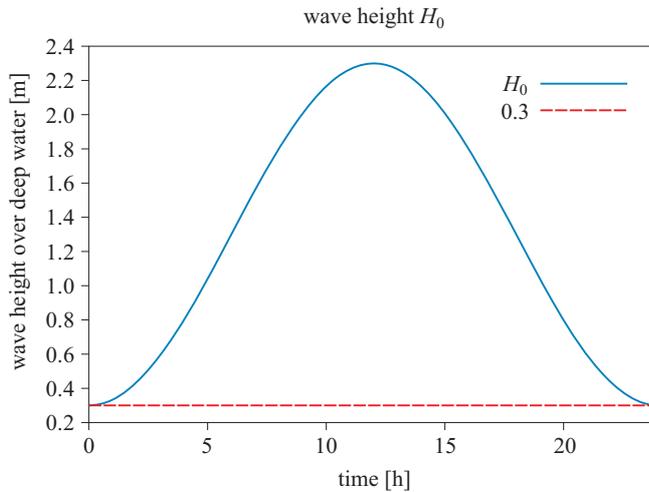
Figure 5. The height of the initialisation wave $H_0(t)$ [m] approaching the shore during a 24-hour storm

The narrow strip of sea, along the coast, between depth H_{br}, where the wave begins to break, and the shoreline is the surf zone.

The experiment of Singamsetti & Wind (1980) shows that the depth at the breaking point H_{br}, the breaking wave height H_{br} and the value γ_{br}

noindent are expressed by the following formulas:

$$H_{br} = 0.575\beta^{0.031} \left(\frac{H_0(t)}{L_0(t)}\right)^{-0.254} H_0(t), \tag{26}$$

$$\left(\frac{H}{h}\right)_{br} = 0.937\beta^{0.155} \left(\frac{H_0(t)}{L_0(t)}\right)^{-0.130}, \tag{27}$$

$$h_{br} = 0.614\beta^{-0.124} \left(\frac{H_0(t)}{L_0(t)}\right)^{-0.124} H_0(t), \tag{28}$$

$$x_{br} = -\frac{h_{br} - 4}{\beta} + 150, \tag{29}$$

$$H_0(t)^2 = H^2 \frac{C_g}{C_{g0}}, \tag{30}$$

$$C_{g0} = \frac{\omega}{k}, \tag{31}$$

$$L_0(t) = \frac{g}{2\pi} T^2, \tag{32}$$

where $H_0(t)$ and L_0 are the height and the length of the wave over deep water respectively.

Determination of the wave height after breaking takes place in the following steps:

- Let us consider, for example, a wave with parameters $H_0 = 0.3$ [m] for the beginning of the storm ($t = 0$) and $T = 6$ [s].

- Using formulas (26) and (28) we determine the depth of the breaking and the wave height at the breaking point, and from relation (29) we calculate the breaking point. Thus we get:
  $H_{br} = 0.53$ [m], $H_{br} = 0.59$ [m] and $x_{br} = 219.49$ [m].

- The coefficients $\Gamma = 0.500$ and $K = 0.175$ depend on the bottom slope, (Dally et al. 1985), and the coefficient $\alpha = 0.684$ is calculated from formula (21).

- Using formula (20) we calculate the wave height $H(x)$ between the breaking point x_{br}, which corresponds to depth H_{br} and the shoreline, where $h = 0$.

Figure 6 shows the changes of the relative wave height $\frac{H}{H_{br}}$ as a function of distance from the shoreline, and Figure 7 presents the changes of parameters (25) of the mean sea level elevation during a storm.

The changes of the characteristic points of the mean sea level elevation during a storm are summarised in Table 1. The table shows that during

Table 1. The effect of changes in storm intensity on variations in mean sea level elevation – as linear and nonlinear approximations

time [h]	$H_0(h)$ [m]	x_{br} [m] Approximation linear	nonlinear	H_{br} [m] Approximation linear	nonlinear	ζ_{br} [m] Approximation linear	nonlinear	$\zeta_{\max}$ [m] Approximation linear	nonlinear	$x_{\max}$ [m] Approximation linear	nonlinear
$t_0 = 0 = t_0 + 24$	0.30	219.86	219.49	0.61	0.61	−0.046	−0.044	0.20	0.140	234.0	232.13
$t_0 + 1 = t_0 + 23$	0.33	218.86	218.46	0.66	0.66	−0.050	−0.047	0.22	0.15	234.4	232.26
$t_0 + 2 = t_0 + 22$	0.43	215.99	215.48	0.81	0.80	−0.058	−0.552	0.26	0.180	235.2	232.66
$t_0 + 3 = t_0 + 21$	0.59	211.590	210.92	1.02	1.01	−0.071	−0.067	0.32	0.22	236.4	233.22
$t_0 + 4 = t_0 + 20$	0.80	206.06	205.19	1.28	1.26	−0.085	−0.080	0.38	0.27	237.6	233.87
$t_0 + 5 = t_0 + 19$	1.04	199.85	198.75	1.55	1.54	−0.100	−0.095	0.46	0.33	239.2	234.54
$t_0 + 6 = t_0 + 18$	1.30	193.37	192.04	1.83	1.82	−0.114	−0.11	0.53	0.38	240.6	235.36
$t_0 + 7 = t_0 + 17$	1.56	187.06	185.50	2.10	2.08	−0.128	−0.121	0.59	0.43	241.8	236.13
$t_0 + 8 = t_0 + 16$	1.80	181.29	179.52	2.33	2.31	−0.140	−0133	0.65	0.48	243	236.82
$t_0 + 9 = t_0 + 15$	2.01	176.42	174.47	2.53	2.51	−0.15	−0.14	0.70	0.51	244.0	237.39
$t_0 + 10 = t_0 + 14$	2.17	172.72	170.64	2.68	2.66	−0.16	−0.15	0.73	0.54	244.6	237.81
$t_0 + 11 = t_0 + 13$	2.27	170.41	168.25	2.77	2.75	−0.161	−0.152	0.75	0.56	245.0	238.08
$t_0 + 12$	2.30	169.62	167.43	2.80	2.78	−0.163	−0.154	0.76	0.56	245.2	238.17
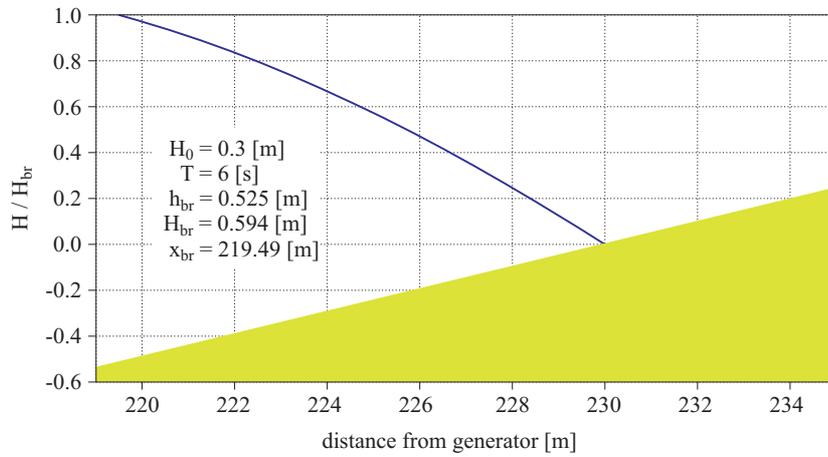
Figure 6. Changes in the normalised wave height function of distance from the shoreline
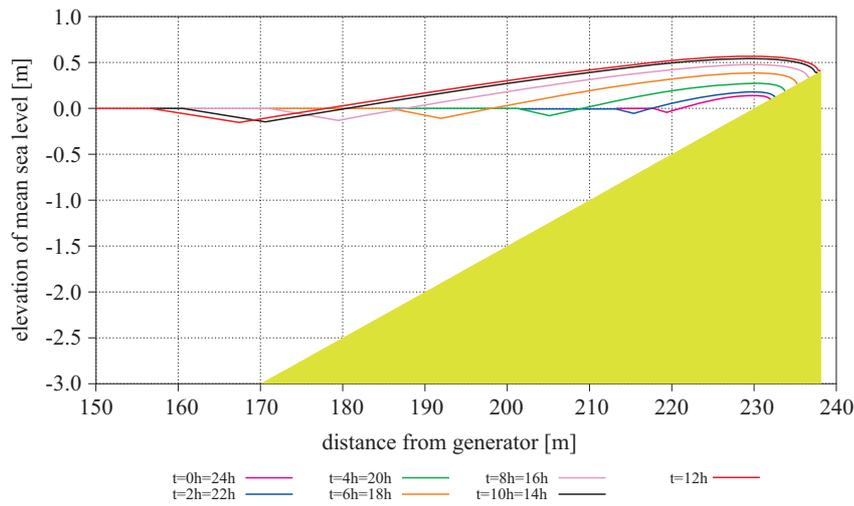
**Figure 7.** Changes in mean sea level rise during the storm

the storm, the height of a breaking wave (H_{br}) over shallowing water depth changes significantly, from 0.61 [m] at the beginning, to 2.78 [m] for time $t = 12h$, when the storm reaches its maximum. Also the place of wave breaking changes from 167.43 [m] with the smallest waves, to 219.49 [m], for the higest waves. As a result of this, extreme nonlinear values of the mean sea level elevation change in the following range:

$$-0.044\,[\text{m}] \ \leq \ \zeta_{\text{br}} \ \leq \ -0.154\,[\text{m}] \ \text{and} \ 0.14\,[\text{m}] \ \leq \ \zeta_{\text{max}} \ \leq 0.56\,[\text{m}].$$

Table 2. The effect of changes in storm intensity on the width of the surf zone –
according to the linear and nonlinear approximations

	Width of the surf zone [m] Approximation	
	linear	nonlinear
$t_0 = 0 = t_0 + 24$	14.14	12.64
$t_0 + 1 = t_0 + 23$	15.54	13.77
$t_0 + 2 = t_0 + 22$	19.21	17.18
$t_0 + 3 = t_0 + 21$	24.81	22.30
$t_0 + 4 = t_0 + 20$	31.54	22.68
$t_0 + 5 = t_0 + 19$	39.35	35.79
$t_0 + 6 = t_0 + 18$	47.23	43.32
$t_0 + 7 = t_0 + 17$	54.74	50.63
$t_0 + 8 = t_0 + 16$	61.71	57.30
$t_0 + 9 = t_0 + 15$	67.58	62.92
$t_0 + 10 = t_0 + 14$	71.88	67.17
$t_0 + 11 = t_0 + 13$	74.59	69.83
$t_0 + 12$	75.58	70.74

Furthermore, the surf zone width (Table 2, Figure 8) changes. As shown
in Figure 3 the width is different for the linear (dependence (17)) and non-
linear relation (24).
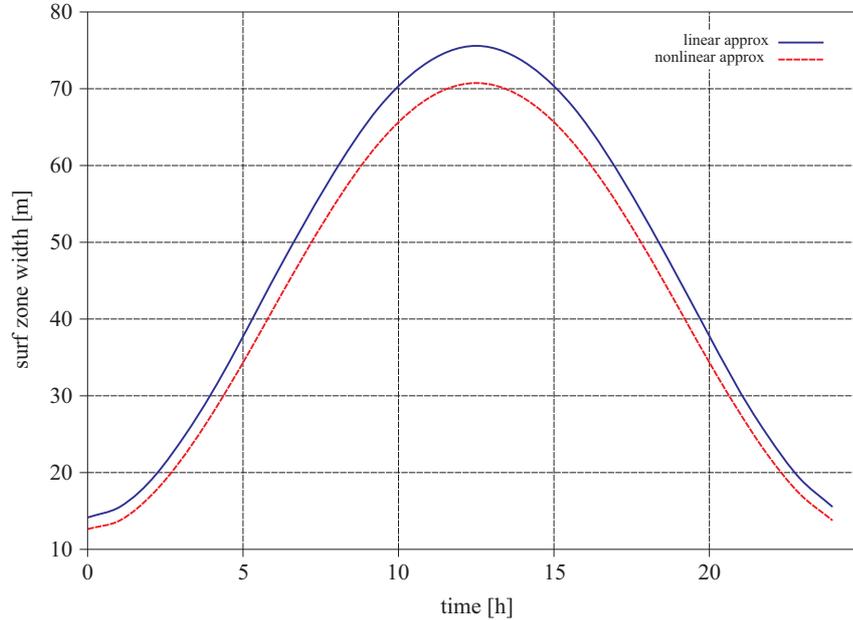
**Figure 8.** Changes in the surf zone width during the storm

3.2. Groundwater flow due to nonlinear set-up

The raising of the mean water level due to the presence of waves causes an additional hydrostatic pressure in the surf zone. This pressure is a driver of water movement in the pore layer.

Massel (2001) presents a theoretical attempt to predict the groundwater circulation due to linear wave set-up. An analogous procedure is applied to the case when the boundary condition is not linear and the mean sea level is assumed after Dally et al. (1985) – see formula (24).

The next step presents the results of calculation of pressure fields and the circulating of pore waters with the assumption of a nonlinear course of the mean sea level elevation.

Figure 9 shows the distribution of pressure and streamlines for a nonlinear mean sea level elevation.
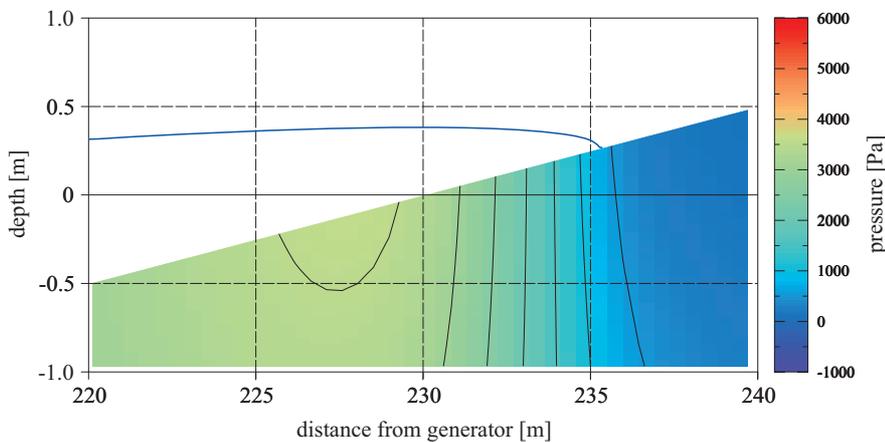

Figure 9. Stream function

Two different systems of water circulation are generated as a result of pressure applied additionally to the bottom. On the left-hand side the impact of the positive pressure gradient driving water movement towards the shore is marked. This means that the pressure gradient is strong enough to overcome the viscosity force in the boundary layer. On the right the second cell of circulation caused by the negative pressure gradient is shown. The line dividing the two systems is formed in the place where the stream function values are zero. This observation is confirmed by the shape of the velocity field in the porous layer (Figure 10).

As seen in Figure 10 water penetrates into porous surfaces in the form of two circulation cells. In both cases, infiltration into the porous medium begins in the vicinity of the place where additionally applied pressure reaches
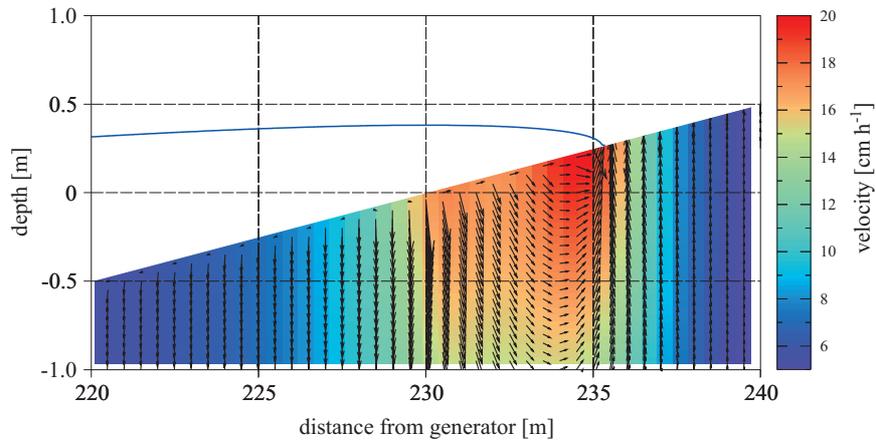
Figure 10. The velocity field in a porous bottom

its maximum value. The outflow is in the lower part of the beach in the first system, and near the water line in the second system. It is worth noting that the second system is much smaller than the first one because the velocity field obtained is not symmetrical in relation to the axis of the local coordinate system.
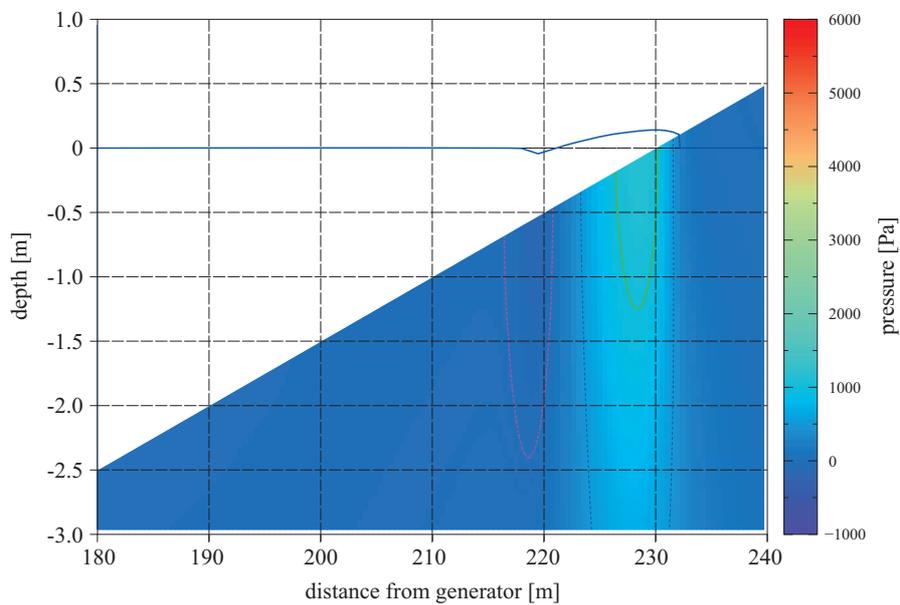
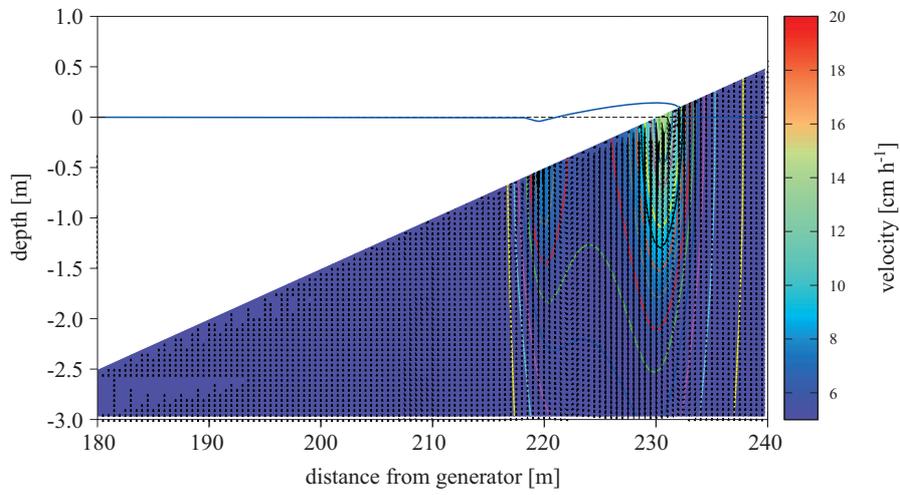**Figure 11.** Pore pressure for time $t_0 = t_0 + 24$ [h]

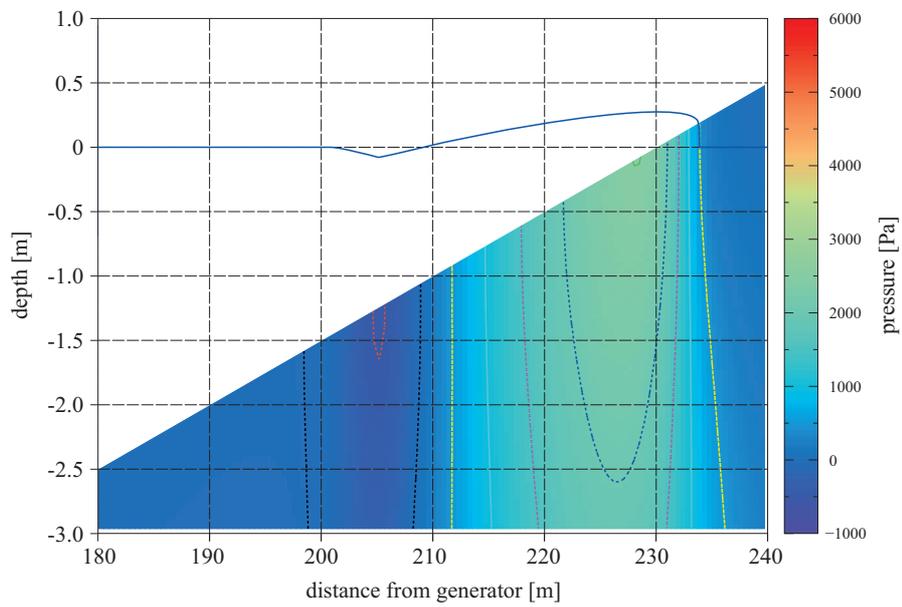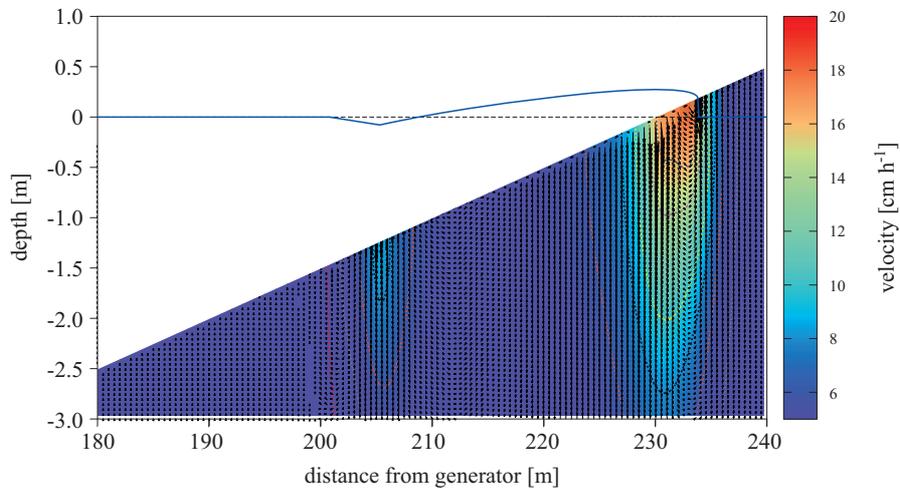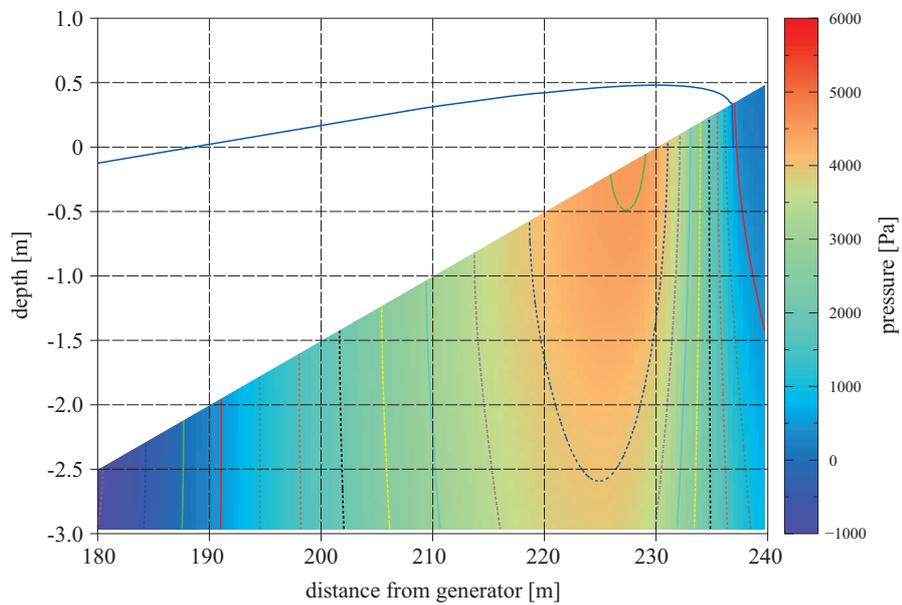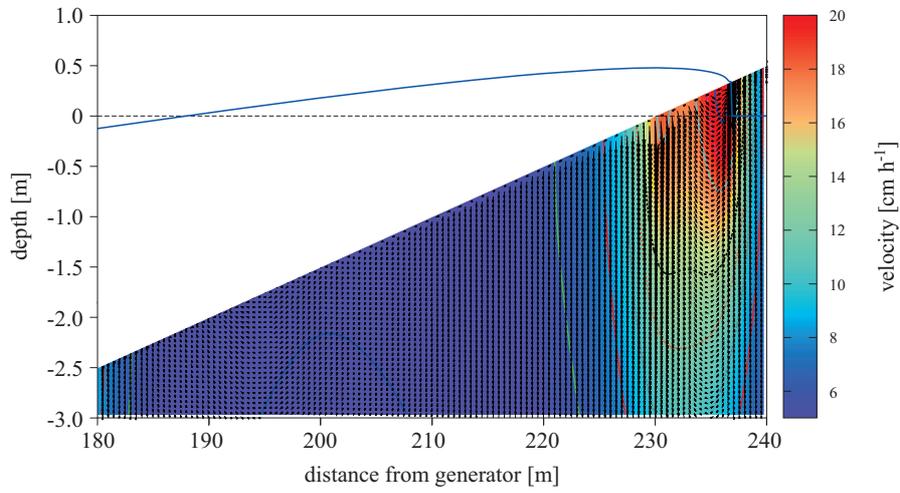**Figure 12.** Pore water velocity for time $t_0 = t_0 + 24$ [h]

Figure 13. Pore pressure for time $t_0 + 4$ [h] $= t_0 + 20$ [h]

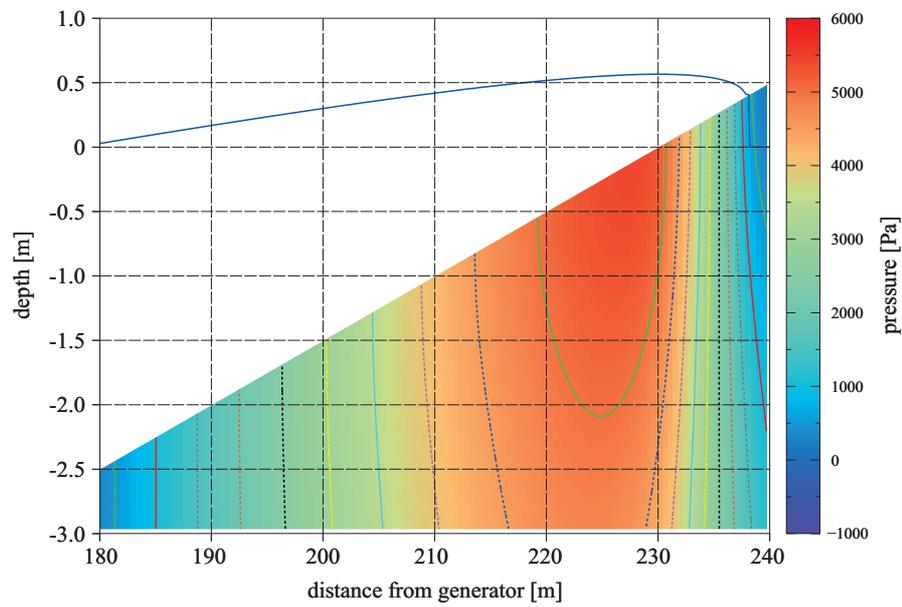**Figure 14.** Pore water velocity for time $t_0 + 4\,[\text{h}] = t_0 + 20\,[\text{h}]$
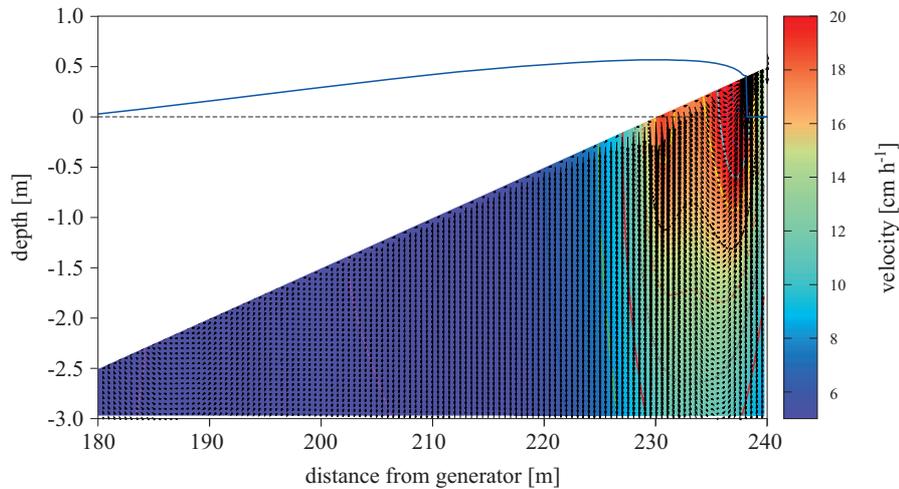
Figure 15. Pore pressure for time $t_0 + 8\,[\text{h}] = t_0 + 16[\text{h}]$

Figure 16. Pore water velocity for time $t_0 + 8 \, [h] = t_0 + 16$ [h]

Figure 17. Pore pressure for time $t_0 + 12$ [h]

Figure 18. Pore water velocity for time $t_0 + 12$ [h]

The resulting changes in pore pressure and pore water velocity, induced by a change in the mean sea level elevation during a 24 [h] hour storm, are illustrated by Figures 11–18.

4. Conclusions

This paper presents a theoretical model attempt to predict the groundwater circulation induced by the nonlinear wave set-up on a permeable beach. The theory is based on the assumption that the phase-averaged, mean pressure gradient, though small, produces effects that, because they are cumulative in time, may be more far-reaching. When a wave breaks, its height decreases and creates a negative pressure gradient which is compensated for by change in mean sea level. In general, the mean sea level elevation set-up is not a linear function. This additional pressure (gradient) is a factor driving the movement of water in the pore layer.

Sea level elevation depends on the characteristics of waves arriving from the open sea. During a storm we can observe very slow changes in the mean sea level elevation over time. The height of a breaking wave above a shallowing bottom changes significantly. Also, the point of wave breaking changes, which results in an extreme non-linear change of mean sea level and of the surf zone width, which is different for the linear and non-linear approximations.

The numerical examples demonstrate the existence of two systems of circulation due to set-up gradients. For the offshore gradient, the

horizontal excess pressure gradient completely swamps the viscous forces in the boundary layer and carries the flow in the offshore direction.

Acknowledgements

References

Biot M. A., 1956, *Theory of propagation of elastic waves in a fluid-saturated porous solid, I. Low frequency range, II. Higher frequency range*, J. Acoust. Soc. Am., 28 (2), 168–191, http://dx.doi.org/10.1121/1.1908241.

Dally W. R., Dean R. G., Dalrymple R. A., 1985, *Wave height variation across beaches of arbitrary profile*, J. Geophys. Res., 90, C6, 11917–11928, http://dx.doi.org/10.1029/JC090iC06p11917.

Holthuijsen L. H., 2007, *Waves in ocenic and coastal waters*, Cambridge Univ. Press, New York, 387 pp., http://dx.doi.org/10.1017/CBO9780511618536.

Longuet-Higgins M. S., 1983, *Wave set-up, percolation and undertow in the surf zone*, Proc. Roy. Soc. London, A390, 283–291, http://dx.doi.org/10.1098/rspa.1983.0132.

Longuet-Higgins M. S., Stewart R. W., 1962, *Radiation stress and mass transport in gravity waves, with application to surf beats*, J. Fluid Mech., 13, 481–504.

Longuet-Higgins M. S., Stewart R. W., 1964, *Radiation stresses in water waves, a physical discussion with applications*, Deep Sea Res., 11, 529–562, http://dx.doi.org/10.1017/S0022112062000877.

Massel S. R., 2001, *Circulation of groundwater due to wave set-up on a permeable beach*, Oceanologia, 43 (3), 279–290.

Massel S. R., Przyborska A., Przyborski M., 2004, *Attenuation of wave-induced groundwater pressure in shallow water. Part 1*, Oceanologia, 46 (3), 383–404.

Massel S. R., Przyborska A., Przyborski M., 2005, *Attenuation of wave-induced groundwater pressure in shallow water. Part 2. Theory*, Oceanologia, 47 (3), 291–323.

Moshagen H., Torum A., 1975, *Waveinduced pressures in permeable sea-beds*, J. Waterway Div., 101, 49–57.

Singamsetti S. R., Wind E. G., 1980, *Breaking waves: characteristics of shoaling and breaking periodic waves normally incident to plane beaches of constant slope*, Delft Hydr. Lab., Rep. M1237, 80.

Verruijt A., 1969, *Elastic storage of aquifers. Flow through porous media*, R. J. M. Deweist, Acad. Press, New York, 331–376.